AUTOMATIC IDENTIFICATION OF CARBONATE KARST CAVES USING A SYMMETRICAL CONVOLUTIONAL NEURAL NETWORK

YUNBO HUANG and JIANPING HUANG

School of Geosciences, China University of Petroleum (East China), Qingdao 266580, P.R. China.
Laboratory for Marine Mineral Resources, Pilot National Laboratory for Marine Science and Technology (Qingdao), Qingdao 266071, P.R. China.
ybhuang95@163.com; jphuang@upc.edu.cn

(Received December 7, 2021; revised version accepted August 21, 2022)

ABSTRACT

Huang, Y.B. and Huang, J.P., 2022. Automatic identification of carbonate karst caves using a symmetrical convolutional neural network. *Journal of Seismic Exploration*, 31: 479-500.

Oil and gas reservoirs with cavities are often developed in carbonate rocks. Accurate karst cave identification is an important step in reservoir interpretation. Traditional methods for karst cave detection are generally performed by searching for the beadlike diffraction phenomena in seismic imaging profiles, which are time-consuming and highly dependent on human interactions. We consider the karst cave detection as an image recognition problem of labeling a 2D seismic image with ones on karst caves and zeros elsewhere. We propose an efficient end-to-end convolutional neural network to automatically identify karst caves from the seismic migration images. To train the network, several velocity models are automatically generated first through our self-defined modeling method, and the karst caves are simulated by adding diffraction points. Then these velocity models are transformed into migration imaging results by finite difference method and reverse time migration. The numerical examples show the stability and capability of the proposed network, which is capable of identifying the karst caves even with the seismic data of different qualities and different frequencies. The physical simulated data example also confirms the effectiveness of our method.

KEY WORDS: karst cave identification, deep learning, finite difference, migration.

0963-0651/22/$5.00

INTRODUCTION

Exploration of hydrocarbon-bearing carbonate formations is of growing interest in the oil and gas industry worldwide, which accounts for approximately half of the world's oil and gas reserves (Gao et al., 2016). Carbonate reservoir has the characteristics of large scale, high yield, and high quality of crude oil and gas. In contrast to sandstones, complex diagenesis, such as dissolution, cementation, and recrystallization, leads to extremely developed karst cave structures in carbonate rocks (Wang et al., 2015). These dissolution caves usually contain a large amount of oil and gas. Therefore, it is very important to quickly identify the karst caves in the seismic interpretation process. Krey (1952) and Hagedorn (1954) find that the diffraction signals in seismic records carry critical subsurface geological information, especially the information of karst caves. The conventional seismic processing techniques mainly focus on the specular reflection waves while the diffraction waves are often ignored or filtered out as interference noise. Even if the diffracted energy can be returned to the place, the diffraction imaging results with relatively weak energy will be contaminated by the strong reflected energy. Therefore, the imaging of diffraction waves separated from the wave field (Kong et al., 2017; Shen et al., 2020) can highlight the energy of underground karst cave structures in imaging (Khaidukov et al., 2004; Zhu et al., 2010; Silvestrov et al., 2016; Berkovitch et al. 2019). However, karst caves are not the only geological bodies that exhibit strong amplitude energy in diffraction wave imaging results, other geological structures such as faults, riverways, and fractures also show similar characteristics. Many efforts have been made to focusing on individually extracting and identifying karst caves from seismic imaging sections. He et al. (2009) propose an accumulation energy difference method for cavern detection in carbonate reservoir by calculating the seismic reflection energy difference in trace or between traces. Liu et al. (2016) combine the edge-based attributes and region-based attributes for caves segmentation from seismic data. The proposed level-set-based framework by integrating two kinds of seismic sttributes can avoids redundant attribute relationships which existed in conventional fusion method. Wang et al. (2017) develops a tensor-based adaptive mathematical morphology to detect and extract the anomalously high-amplitude bright spots on seismic migration images. Fan et al. (2017) construct a new cave recognition operator for karst cave identification by using the GST theory and the geometrical features of the dissolution karst. Other studies try to establish the correspondence between the karst caves and its seismic imaging features, to help the interpreters better describe the cavities. Qu et al. (2012) derives the analytic expression of seismic response for an small isolated karst cave based on the acoustic wave equation under the premise of ignoring multiple scattering. Xu et al. (2016) conduct a physical modeling experiment to understand the beadlike diffraction features of karst caves with different scale, velocity, shape and fluids. These traditional karst cave identification methods either require a lot of computation costs or manual interpretation.

Therefore, an efficient, robust, and atomatic karst cave identification technique is appealing.

In recent years, deep learning has achieved state of art in many fields and has obtained good results in solving problems that require human intervention. Many efforts have been also made to seismic data processing using deep-learning technologies. For instance, Wu et al. (2019) propose an end-to-end supervised deep learning network for automatic fault segmentation. Shi et al. (2018) embed U-Net into the recurrent neural network to precisely detect the salt bodies, where the predicted salt dome boundary is more accurate. Yang and Ma (2019) implement a fully convolutional neural network to learn the nonlinear mapping between the shot data and seismic velocity models. Gao et al. (2020) design a novel deep learning network with double input to classify the flow structures and characterize the gas void fraction. Huang et al. (2020) apply a convolutional neural network to change the raw seismic data into a local slope map. For the automatic identification on karst caves, Cai et al. (2018) present an improved deep learning model using the optimized convolutional nearal network to identifying karst caves. This method only detects karst caves, does not accurately characterize the shape of the caves, and the labels of the training data are manually calibrated on the physically simulated dataset.

In this study, we develop a convolutional neural network (CNN) for automatic karst cave identification directly from migration images The original U-net architecture (Ronneberger et al., 2015) is modified to be more suitable for the automatic cavity identification problem. A boundary padding operation is added into each convolutional layer of the original U-Net to ensure that the input and output are of the same size. Considering that the binary label is highly unbalanced with a dominant distribution of zeros (non-karst caves) but only a very small proportion of ones (karst caves), we use a class-balanced cross-entropy loss function to maintain good convergence during the training process. To generate the velocity models with karst caves under different geological structures and background velocities, we design a set of automatic generation methods of the karst cave velocity models. The diffraction points with different scales and velocities are used to simulate the karst caves and the velocity models with karst caves are generated by randomly adding the diffraction points to the velocity models. Through the finite difference method (Ozdenvar and McMechan, 1997; Hardi and Sanny, 2016) and reverse time migration (Baysal et al., 1983; Chang, 1987), these velocity models with karst caves are transformed into the migration images, which are the inputs of the CNN. The label is a probability distribution map of karst caves, which is a binary image, with 1 representing karst caves and 0 representing non-karst caves. Namely the automatic karst cave identification problem is turned into a dichotomy problem. During the training process, the migration images are fed into the network together and the network effectively approximates the nonlinear mapping between the seismic data and the corresponding probability distribution of karst caves.

Although the training process is expensive, the cost of the prediction stage by the network is negligible once the training stage is completed. One migration image of the testing data sets can be predicted within 1 s by the well-trained model, which is performed on the workstation with NVIDIA RTX5000 GPU. Sensitivity tests on data sets generated with different imaging quality, wavelet frequency, and incorrect migration velocity are performed. The prediction results on the physical simulated data also demonstrate the applicability of our method..

This paper is organized as follows. We first present the data preparation method, including the automatic generation of the velocity models with karst caves and the generation of migration images and the corresponding labels. Then we illustrate the network architecture for karst cave identification in detail. We perform sensitivity tests on imaging qualities, wavelet frequency and migration velocity errors. We also verify our method on a physically simulated dataset. Finally, we discuss the identification performance of the proposed network, advantages, disadvantages, and improvement methods.

TRAINING DATA SETS

There are three types of machine learning, supervised learning, semi-supervised learning, and unsupervised learning. For an image recognition problem, the most effective way is supervised learning, namely, the true labels are known during the training process. However, the true labels can not be obtained for many geophysical problems. For the case of karst cave identification, labeling karst caves manually is time-consuming and subjective, and sometimes may lead to incorrect labels. Inaccurate or even wrong labels will affect the training process of the neural network and reduce the accuracy of the prediction results. To address these issues, we propose a method to automatically generate the velocity model with karst caves by establishing an accurate relationship between the karst caves and the migration imaging results from the wave-field response characteristics. The data set for network training is generated based on the wave equation.

Automatic velocity model generation

To train an efficient network, it is necessary to simulate the migration imaging characteristics of the karst caves under various geological and structural background conditions. Therefore, we first create a certain number of velocity models without karst caves. The automatic modeling strategy was inspired by the data augmentation approach for automatic fault segmentation in Wu et al. (2019). In this workflow, we first create the horizontal layered velocity models with different thicknesses of each layer, with the velocity values of each layer ranging from 2000 to 6000 m/s. Then,

we increase the complexity by vertically shearing the velocity model. As shown in Fig. 1, we define four types of models including horizontal layered models with velocity gradually increased with depth, curved layered models, models featured with thick and reverse layers, and models with a high-speed anomaly. All the automatically generated velocity models have the same size of 512×256 points. A total of 55 different velocity models are automatically generated during this process.

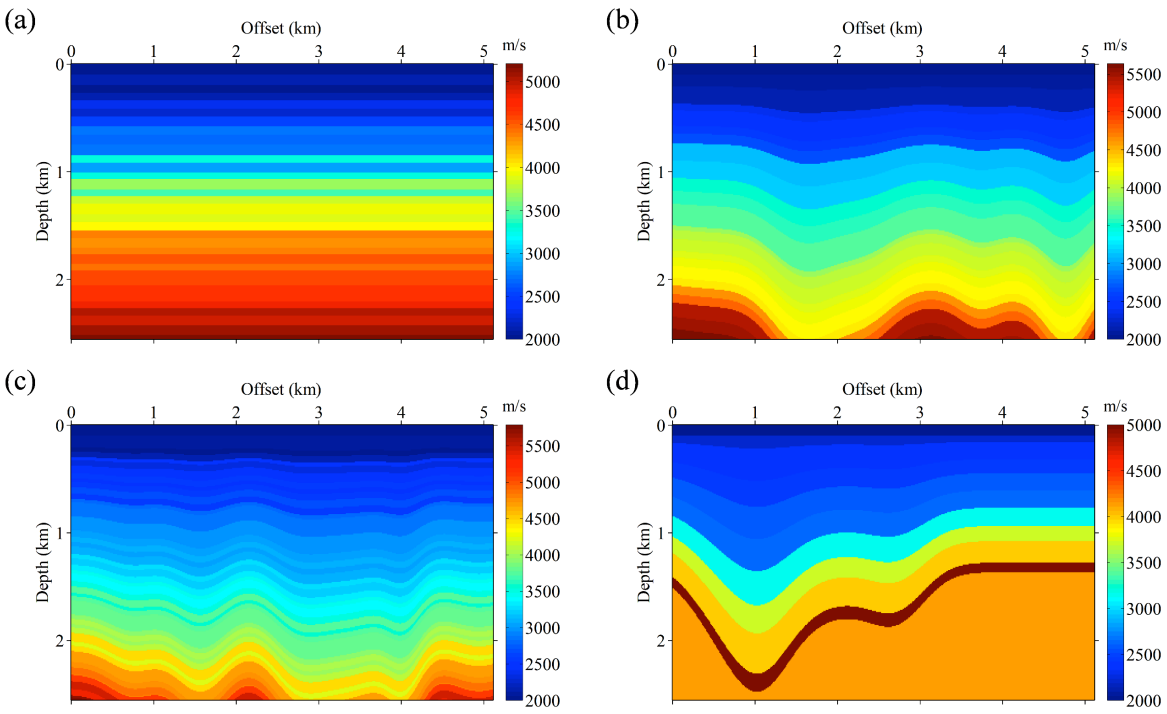

Fig. 1. Four self-generated velocity models with different geological structures in a total of 55 models. (a) represents the horizontal layered models; (b) refers to the curved layered models; (c) represents the models featured with thick and reverse layers; (d) is the models with the high-speed anomaly.

Adding diffraction points

We add diffraction points to the velocity models to generate models with karst caves. To simulate karst caves of different sizes, we generate three types of diffraction points with different pixels, 1×1, 2×2, and 3×3. For each generated velocity model, 100 diffraction points with different positions and sizes are randomly added. The velocity values of the karst caves are given by adding a random perturbation to the original velocities and the perturbation value is -0.33 to 0.33 times the originals. The label is a probability distribution map of karst caves, which is a binary image, with 1 representing cavities and 0 representing non-cavities. Fig. 2 shows four representative velocity models with diffraction points, from which the corresponding binary labels are (Fig. 3) obtained easily.

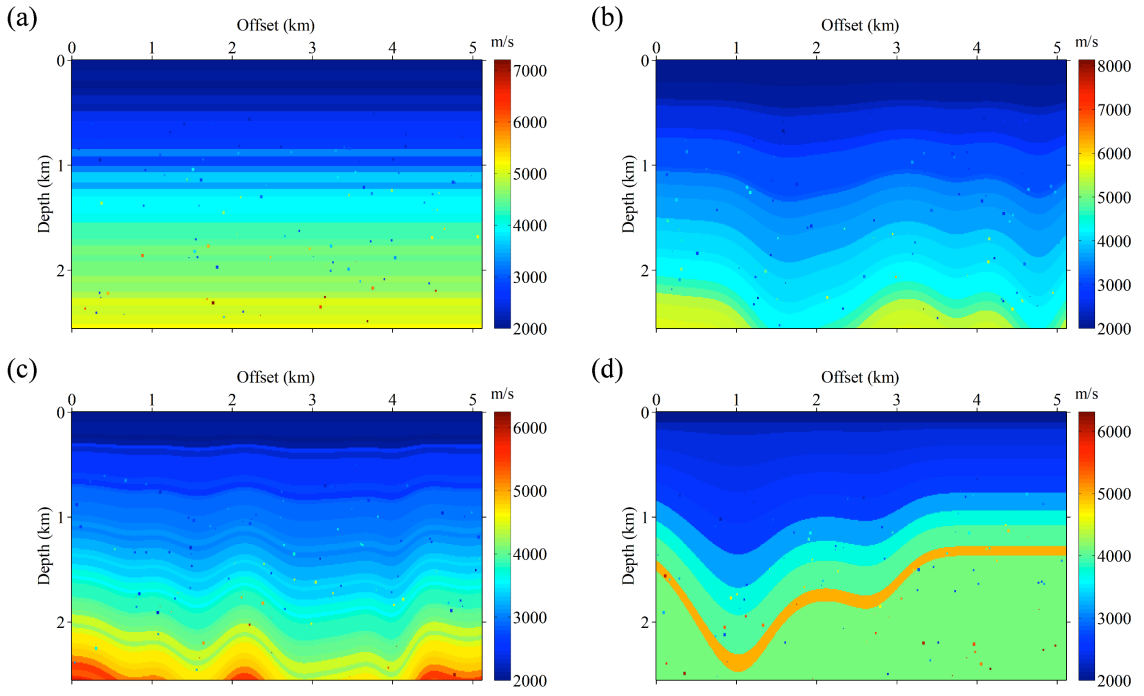

Fig. 2. Four representative velocity models with karst caves, generated by adding diffraction points to the velocity models in Fig. 1.

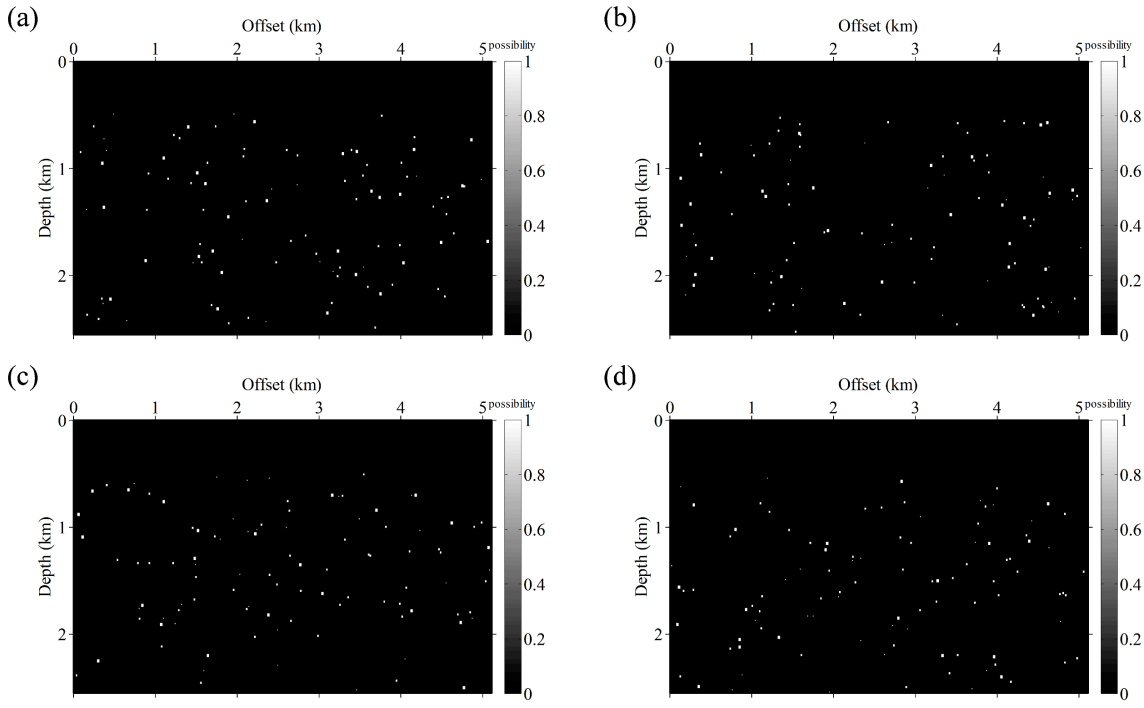

Fig. 3. The labels correspond to the velocity models with karst caves in Fig. 2. The white spots in the binary images denote karst caves (ones) and the elsewhere black area represents non-karst caves (zeros).

Migration image generation

We focus on automatic karst cave identification from the migration imaging profiles. The network takes in the migration imaging results and outputs a 2D karst cave distribution probability map. The velocity models with karst caves and the corresponding probability distribution map of karst caves are generated, the migration imaging results corresponding to these velocity models are required to be generated for preparing the input data set. We use the finite difference method to simulate seismic waveforms with a 30 Hz Ricker wavelet. For each velocity model, 50 sources are evenly placed with a spatial interval of 100 m and 512 receivers are evenly placed with a spatial interval of 10 m. To simulate more realistic imaging results, we add random noise to the shot records before performing the migration process. After forward simulation, these generated velocity models are smoothed to be the migration velocity models. We perform reverse time migration and Laplace filtering (Burt and Adelson, 1983) to obtain the 55 final migration imaging results (Fig. 4).

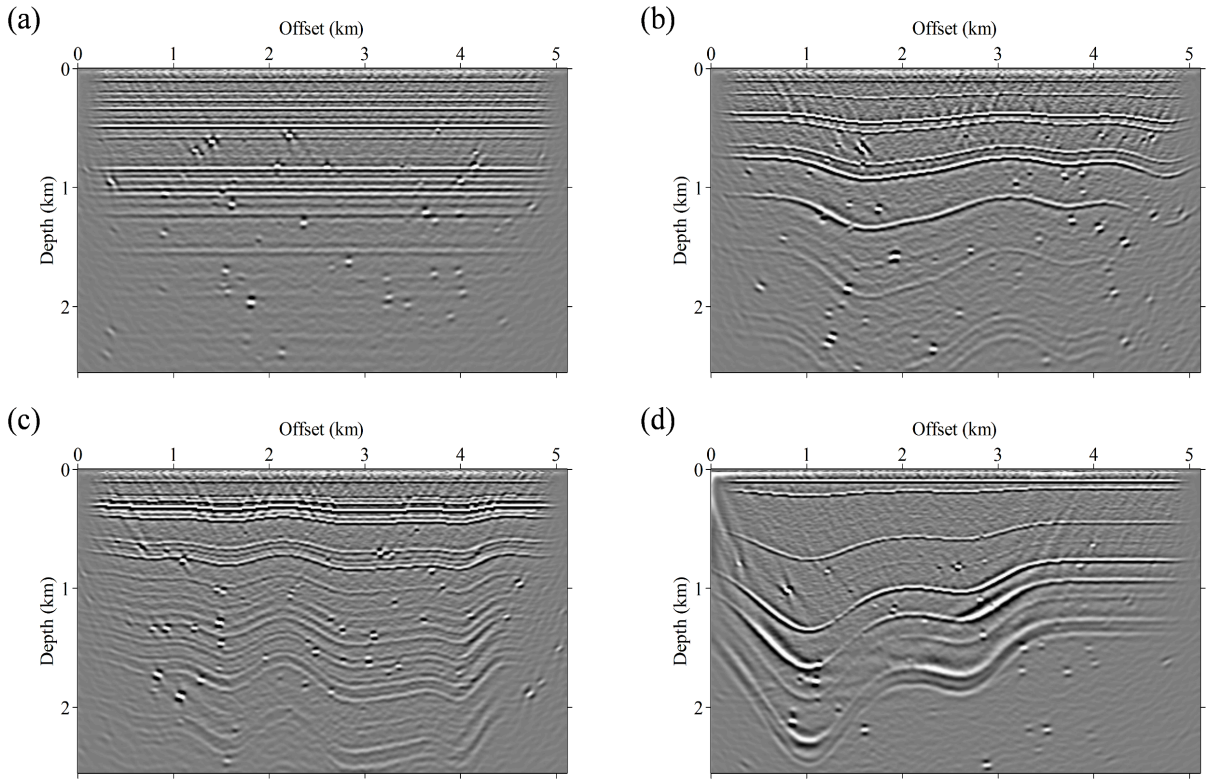

Fig. 4. The reverse time migration images generated with the finite difference method from the velocity models in Fig. 3. High-pass filtering is performed to decrease the low-frequency noise.

CNN-BASED KARST CAVE DETECTION METHOD

In this section, we first illustrate the network architecture for karst cave identification in detail. Then, a class-balanced binary cross-entropy loss function (Xie and Tu, 2015) is presented.

Network architecture

U-Net is an auto encoder-decoder network designed for medical image segmentation. As shown in Fig. 5, the main structure of the network includes two parts, down (encoder) and up (decoder). Both the input and output are images. The shallower layer is used to solve the pixel positioning problems, whereas the deeper layer is responsible for pixel classification.

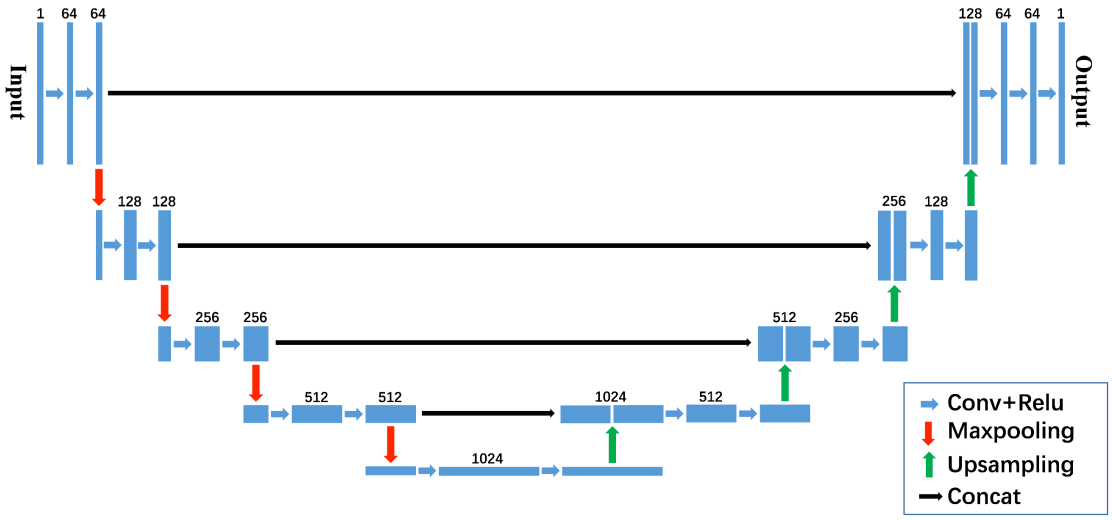

Fig. 5. A modified convolutional neural network (U-Net) for automatic karst cave detection.

The network contains a total of 23 convolutional layers. In the contracting path on the left, each step includes two 3×3 convolutional layers followed by a ReLU activation (Nair and Hinton, 2010; Krizhevsky et al., 2012) and a 2×2 max-pooling operation with stride 2 for downsampling. Symmetrically, each step on the right expansive path consists of a 2×2 upsampling operation with the same stride, and two convolutional layers to halves feature channels. In each step, the concatenation path links the left and right paths to recover the spatial information damaged mainly by max-pooling and other operations. The sigmoid activation function is applied to the last channel feature vectors to produce a probability map of the output with the same size as the input. The network contains four times of upsampling operation in total and the skip connection is used in the same stage instead of directly monitoring and loss back-transmission on high-level

semantic features. In this way, more low-level features are integrated into the finally recovered feature map. It also enables the integration of features of different scales, so that multi-scale prediction and deep supervision can be carried out.

Class-balanced cross-entropy loss

The loss function represents the difference between the true karst caves and the predictions, which is very important for network training. The update of the parameters in the network is achieved through the loss backpropagation (Hecht-Nielsen, 1989) during the training process. We regard the karst cave identification problem as a binary segmentation problem. The output of the network is a probability distribution of 0-1. The binary cross-entropy loss function is generally used in the binary segmentation of a common image:

$$Loss = -\sum_{i=1}^{n} (y_i \times \ln x_i + (1 - y_i) \times \ln(1 - x_i)), \tag{1}$$

where n represents the number of pixels. y_i denotes the true binary labels (0 or 1) and x_i is the prediction probabilities ($0 < y_i < 1$) computed from the sigmoid activation in the last convolutional layer. The proportion of karst caves in the whole imaging region is relatively small, resulting in the highly imbalanced between zeros (non-karst caves) and ones (karst caves). To address this issue, we use a class-balanced binary cross-entropy loss function (Xie and Tu, 2015) to avoid the situation that the network is not trained or converged to predict only zeros.

$$Loss = -\sum_{i=1}^{n} (\beta \times y_i \times \ln x_i + (1 - \beta) \times (1 - y_i) \times \ln(1 - x_i)), \tag{2}$$

where $\beta = Y_0 / Y$ and $1 - \beta = Y_1 / Y$. Y_0 and Y_1 denote the number of pixels of karst caves and non-karst caves in the label data sets, respectively. Y represents the total number of pixels in the label data sets. By introducing the class-balancing weight β on a per-pixel term basis, the binary cross-entropy loss with additional trade-off parameters for biased sampling can help the network converge in the correct direction.

Training and testing

We generate a total of 55 migration images and the corresponding labels, then we divide the inputs into 64×64 sample patches having 2750

patches in total. We assign 2475 and 275 samples as the training and validation data sets, respectively. Fig. 6 is a partial display of the data set we used to train the network. The first column shows the velocity models, the second column shows the corresponding migration images (inputs), and the third column is the karst cave probability distribution maps (labels). To test the effectiveness of our method, we create two new velocity models with karst caves based on the section of the BP 2.5D model and Marmousi model and convert these two new models into migration images using the same process. The testing data set are different from the training data set and are unknown during the prediction process.

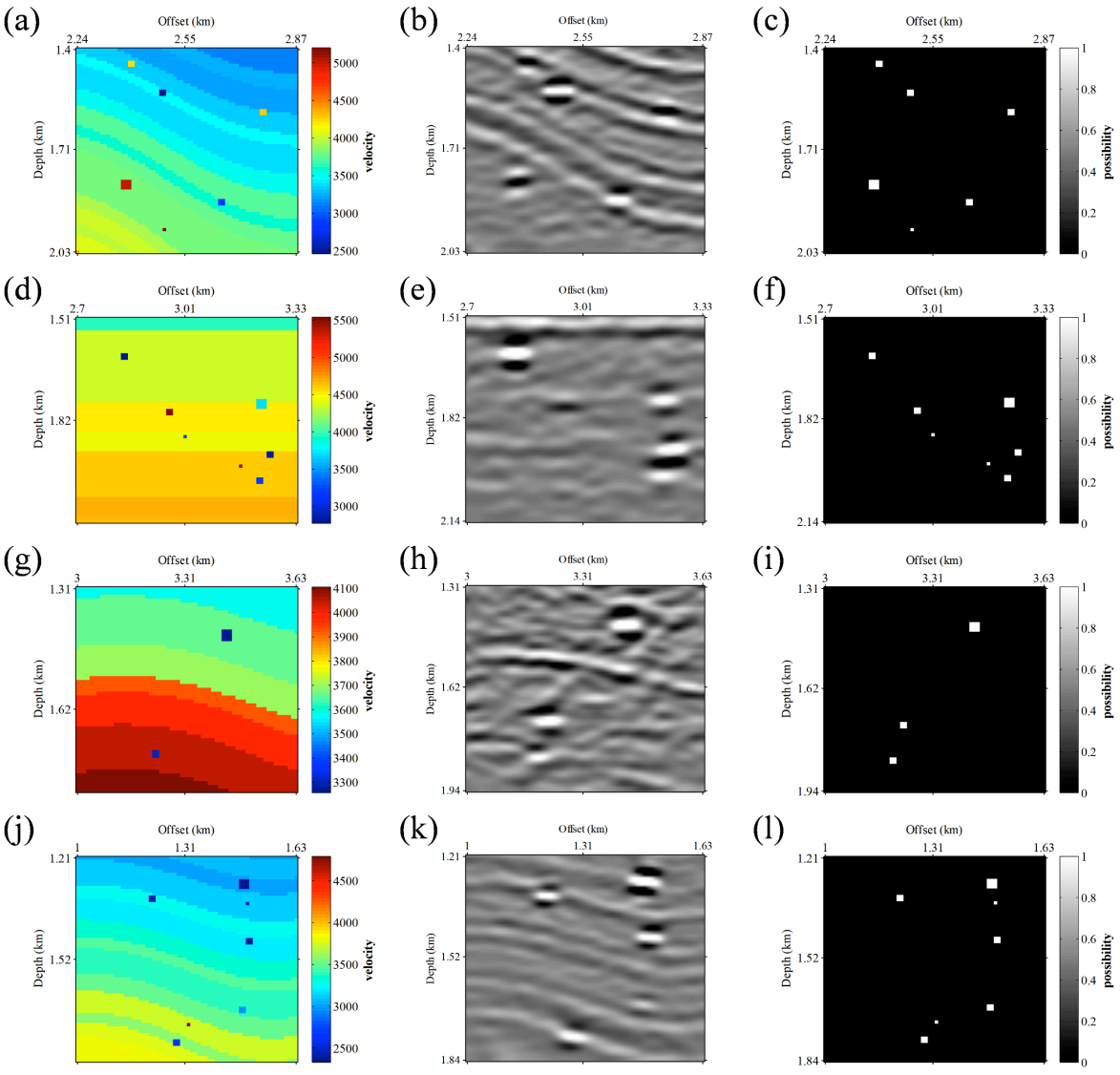

Fig. 6. Samples from training data set and corresponding velocity model sections. The first column is the velocity models, the second column represents the corresponding migration images as inputs, and the third column shows the karst cave probability distribution maps as the labels.